European Journal of Pharmaceutics and Biopharmaceutics 75 (2010) 263–276

Contents lists available at ScienceDirect

European Journal of Pharmaceutics and Biopharmaceutics

journal homepage: www.elsevier.com/locate/ejpb

Research paper

Synchrotron X-ray microtomographic study of tablet swelling

P.R. Laity *, R.E. Cameron

Department of Materials Science and Metallurgy, University of Cambridge, Cambridge, UK

ARTICLE INFO

Article history:
Received 15 November 2009
Accepted in revised form 15 February 2010
Available online 19 February 2010

Keywords:
X-ray microtomography (XμT)
Tablet
Swelling
Hydroxypropyl-methyl-cellulose (HPMC)
Pre-gelatinised starch (PGS)
Microcrystalline cellulose (MCC)
Gel forming

ABSTRACT

Tablet swelling behaviour was investigated by following the movements of embedded glass microsphere tracers, using X-ray microtomography (XμT) with intense illumination from a synchrotron. Specimens were prepared using combinations of hydroxypropyl-methyl-cellulose (HPMC) and microcrystalline cellulose (MCC) or pre-gelatinised starch (PGS), three materials commonly used as excipients for compacted tablets. The results revealed significant differences in swelling behaviour due to excipient type and compaction conditions. In particular, a sudden change was observed from gel-forming behaviour of formulations containing PGS or high HPMC content, to more rapid expansion and disintegration for formulations above 70% MCC. Although some radial expansion was observable with the higher PGS formulations and during later stages of swelling, axial expansion (i.e. the reverse of the compaction process) appeared to dominate in most cases. This was most pronounced for the 10/90 HPMC/MCC specimens, which rapidly increased in thickness, while the diameter remained almost unchanged. The expansion appeared to be initiated by hydration and may be due to the relaxation of residual compaction stress. This occurred within 'expansion zones', which initially appeared as thin bands close to the compacted (upper and lower) faces, but gradually advanced towards the centre and spread around the sides of the tablets. These zones exhibited lower X-ray absorbance, probably because they contained significant amounts of bubbles, which were formed by air released from the swelling excipients. Although, in most cases, these bubbles were too small to be resolved (<60 μm), larger bubbles (diameter up to 1 mm) were clearly evident in the rapidly swelling 10/90 HPMC/MCC specimens. It is suggested that the presence of these bubbles may affect subsequent water ingress, by increasing the tortuosity and occluding part of the gel, which may affect the apparent diffusion kinetics (i.e. Fickian or Case II). These observations also suggested that axial expansion, initiated by water ingress, may be an important mechanism during tablet swelling.

1. Introduction

Gel-forming tablets provide a popular and convenient 'sustained-release' dosage form for delivering drugs over an extended time [1–6]. The drug is dispersed within a polymeric matrix, which controls the release rate. In contrast to 'burst-release' tablets, which disintegrate rapidly when swallowed and release their pharmacologically active ingredients instantly, gel-forming tablets swell gradually, allowing the drug to escape slowly from the polymer matrix, by diffusion or erosion, over several hours. This can provide several potential benefits: sustained-release can provide a less variable drug concentration in the patient's body, which maintains efficacy while avoiding adverse side effects associated with concentration spikes; also, 'sustained-release' tablets need to be taken less frequently, which may improve compliance.

Typically, gel-forming tablets are based on a small set of pharmaceutically acceptable, water-soluble polymers, including cellulose ethers, such as hydroxyethyl-, hydroxypropyl- and hydroxypropyl-methyl-cellulose (HPMC), modified starches and a few synthetic polymers, such as poly(ethylene-oxide) and poly(vinyl-pyrrolidone). These may be used singly or in combination with other excipients, to modify the compaction and swelling behaviour of the formulations.

A considerable number of techniques have been developed to study the swelling and drug-delivery characteristics of these systems [7], ranging from simple measurements of drug release into the surrounding liquid [8–15] and various optical methods [15–20], to sophisticated diffusometry- or relaxometry-based experiments using magnetic resonance imaging (MRI) [21–37]. The results reveal a set of interrelated mechanisms that operate following immersion of the tablet in water.

Firstly, within one minute, a small amount of water rapidly penetrates a short distance into the tablet; this allows particles of the dry excipient near the tablet surface to swell into a gel [18,19] that blocks pores and controls the subsequent ingress of water. Further water penetration occurs by diffusion, apparently following Fickian

* Corresponding author. Pfizer Institute for Pharmaceutical Materials Science, Department of Materials Science and Metallurgy, University of Cambridge, Pembroke Street, Cambridge CB2 3QZ, UK. Tel.: +44 1223 767059; fax: +44 1223 334567.
E-mail address: prl28@cam.ac.uk (P.R. Laity).

0939-6411/$ - see front matter © 2010 Elsevier B.V. All rights reserved.
doi:10.1016/j.ejpb.2010.02.009

(i.e. progressing with the square-root of time) [17,28–32,36], Case II (i.e. progressing linearly with time) [30–35], or anomalous diffusion (i.e. intermediate between Fickian and Case II) [34] depending on the tablet composition and swelling conditions, such as pH [30,31]. This produces a 'swelling' or 'hydration' front between the hydrated outer regions of the tablet and the dry excipient within the tablet core. Simply measuring the movement of this front may be misleading, however, since the advance due to diffusion may be countered by an expansion of the core in the axial direction [15,19,23,26,27,37], which is usually attributed to the relaxation of residual compaction stress.

Where sufficient water has penetrated, the excipients form a gel layer, consisting of swollen polymer and any other dissolved or suspended materials from the tablet. The thickness and composition of this gel depend on the relative rates of adding more dry material from the tablet core (at the hydration front), dilution by water diffusing into the gel and erosion from the outer gel–liquid interface (i.e. the erosion front). Hence, its properties can be affected by the type of polymer [16,32,33], the presence of any other tabletted materials (i.e. excipients or drugs [14,15,29,31]) and the composition of the swelling medium. The gel becomes progressively more dilute towards the bulk liquid, which results in longer nuclear relaxation times and faster diffusion rates [21–24,27–33,37]. Drug release is controlled by this gel layer and can occur by two mechanisms [7], depending on the solubility of the drug. At some point within the swollen gel (the dissolution front), readily soluble drugs start to dissolve and diffuse out [16,29]; otherwise, less soluble drugs are released at the erosion front.

We recently demonstrated a further addition to these methods, using X-ray microtomography (XμT) to observe the movements of tracer particles embedded within the gel-forming tablet [37]. This provided a method for observations in three-dimensions, analogous to the essentially two-dimensional method reported previously be Adler et al. [20]. Swelling and gel formation were revealed by the movements of tracers that started close to the tablet surfaces. Moreover, in contrast to MRI, which requires a sufficient water concentration within the material to lengthen the relaxation times associated with the nuclear spin magnetisation and provide an observable echo signal above any background noise [21–23,37], the XμT method was also able to show any movements within the relatively dry interior of the tablet. This revealed a 'mechanical relaxation' in the axial direction, within the tablet interior, ahead of the advancing hydration fronts that marked the (inward moving) limit of the MRI signal [37].

The present work employed the XμT method to study the swelling behaviour of a range of gel-forming formulations based on HPMC and mixtures with microcrystalline cellulose (MCC) or pre-gelatinised starch (PGS). Using the intense X-ray illumination from a synchrotron permitted relatively rapid acquisition of good quality images, compared with the bench-top tomograph used in our previous work [37]. Hence, the present study has mainly concentrated on the earlier stages of swelling.

2. Materials and methods

HPMC (Methocel K4M premium EP, Colorcon Ltd., Kent, UK), PGS (1500, Colorcon Ltd., Kent, UK) and MCC (Avicel PH101, FMC Corp., USA) were stored under ambient conditions and used as received. Specimens were produced from single powders or mixtures, as indicated in the text. In each case, the powder was mixed with glass microspheres (Jencons, UK, sieved diameter 180–212 μm, approximately 1% by weight), by tumbling in a turbula mixer (Willy A Bachofen AG, Switzerland) for at least 15 min.

The powder charge (0.40–0.41 g) was transferred to an unlubricated stainless steel die (10 mm internal diameter, Specac Ltd., Smiths Industries, Kent, UK). Single-sided compaction was performed, using a mechanical testing rig (Instron Ltd., High Wycombe, Buckinghamshire, UK), at a speed of 3 mm min^{-1} during loading to the chosen maximum force and unloading. The specimen was ejected immediately after unloading, in the same direction as the compaction; its diameter (d_0) and height (h_0) were measured using callipers with a vernier scale (to ±0.02 mm), within 1 min of ejection; its weight was subsequently measured using a top-pan balance (to ±0.0003 g), in order to estimate the bulk density. The compositions and relative densities of the specimens used in this work are summarised in Table 1. The upper surface of each specimen was numbered using a soft pencil, in order to identify both the specimen and its compaction direction.

XμT experiments were performed on beamline ID19, of the ESRF, Grenoble, using an effectively parallel beam of monochromatic X-rays of 30 keV and with a sample-to-detector distance of 30 mm. For each acquisition, 500 projection images with exposure time of 50 ms were collected using a fast readout-low noise (FReLoN) CCD camera [38,39]. The field of view (FoV) of 30 × 10.7 mm was resolved into 980 × 350 pixels, giving a spatial resolution of 30.6 μm $pixel^{-1}$ in both horizontal and vertical directions. Light-field images (i.e. X-ray illumination on and the specimen out of the beam-path) and dark-field images (i.e. X-ray illumination off) were also collected during each acquisition procedure, in order to correct for electronic noise and variations in the X-ray source brightness. Including the time required for data-transfer, each acquisition took 2.36 min.

Swelling experiments were performed inside a clear plastic sample vial, which was mounted on the beamline sample stage. Specimens were placed singly into the vial, on a plastic support and immersed in distilled water. After performing the usual safety checks, the experimental hutch was secured, before a series of pre-programmed acquisitions was started; this resulted in a delay of about 80 s from the start of swelling, so that the mid-point of the first acquisition was at about 2.5 min. Most experiments were restricted to the early stages of swelling (up to about 70 min), although a few were allowed to continue up to 6 h.

Sets of projected images, corresponding to each time-point within the swelling experiment, were reconstructed using pyHST software written at the ESRF to perform a direct filtered back-projection algorithm. This produced 'stacks' of 980 × 980 × 350 cubic voxels (i.e. the 3D equivalents of pixels, of size 30.6 μm in each direction), which comprised a sequence of horizontal slice images. Subsequent analyses and measurements were performed using Image-J software [40]. For each swelling experiment, a region of interest (RoI) was selected manually around the tablet diameter (typically, 30 or 40 voxels thick, i.e. spanning 15 or 20 voxels either side of the diameter, depending on the abundance of glass microspheres), of sufficient width (480 voxels) and height (350 voxels), so that the tracers remained within this region throughout swell-

Table 1
Composition and relative densities for specimens used in this work (uncertainty estimate shown in first row).

Composition (w/w)	Compaction pressure (MPa)	Relative density
100% HPMC	64	0.849 ± 0.006
100% HPMC	127	0.896
100% HPMC	318	0.940
90% HPMC + 10% MCC	127	0.906
70% HPMC + 30% MCC	127	0.897
30% HPMC + 70% MCC	127	0.885
10% HPMC + 90% MCC	127	0.884
60% HPMC + 40% PGS	127	0.889
40% HPMC + 60% PGS	127	0.878
20% HPMC + 80% PGS	127	0.874
10% HPMC + 90% PGS	127	0.869

ing. Each 'peri-diametral' RoI was 're-sliced' and 'projected' into a single (vertical) image. It was found that different features could be enhanced using 'Image-Stacks-Z Project' and selecting the projection options (i.e. average, maximum or minimum intensity), which are built into the Image-J software. These options produced an image containing pixels using the average, brightest or darkest values from a corresponding row of voxels through the RoI; choosing 'minimum intensity' revealed the tracers, while 'maximum intensity' revealed regions of low density and bubbles. The images were further enhanced by applying false colour (shown in the 'online' version of this paper). Generally, the greyscale range was chosen so that white indicated complete transmission, while black indicated the strongest absorbance within the set of acquisitions for that experiment (i.e. still less than total absorbance, which would have compromised the tomographic reconstructions). In some cases, however, this range was restricted further, to increase contrast and reveal specific features.

3. Results

A typical sequence of images demonstrating the swelling of a HPMC tablet specimen over 5.3 h is shown in Fig. 1. (Note: the fuzzy, vertical lines through the middle of these and other XμT images are artefacts.) Due to the stronger X-ray absorbance of the glass microspheres compared with water or HPMC, they appeared as small dark circles, which could be revealed by 'projecting' voxels of minimum intensity through the selected (30 voxel thick) 'peri-diametral' RoI. The two dark shapes at the bottom of each image are due to the plastic support beneath the specimen.

The specimen appeared to rise off the supports, as swelling progressed; this was caused by gel forming ahead of the outermost tracers. Due to the relative hardness of the glass and the steel compaction die, compared with the pharmaceutical excipients used here, the centre of each microsphere was expected to lie at least one radius distance (approximately 100 μm) from the geometric surface of the specimen. It is likely, therefore, that HPMC closer to the surface could swell without the movement of nearby microspheres. Hence, as noted previously [37], the movements of the outermost tracers indicated the expansion as the tablet swelled, but not the absolute limits of the polymer gel.

The region containing the glass microspheres gradually expanded over the course of the swelling experiment. In order to facilitate comparison, a rectangle has been superimposed onto each frame, centred on the region containing the relatively static tracers within the tablet core (hence, tracking the upward movement during swelling) and roughly indicating the initial size of the specimen prior to swelling. Hence, it can be seen that the expansion did not take place equally in all directions; although a small amount of radial expansion was evident during the later stages (from 72 min onwards), vertical (i.e. axial) expansion started sooner (from 14 min) and predominated throughout these swelling experiments. This was consistent with observations by other workers using optical methods [15,19], MRI [23,26,27] and our own previous findings based on a combination of MRI and XμT [37]. To put this expansion in context, during the preparation of these specimens, elastic recovery of typically 0.25 ± 0.01 mm was observed when the compaction force was removed (i.e. spring-back during unloading); by contrast, axial expansion in excess of 0.5 mm was observed during the first 30 min of swelling, with no indication of the process slowing down.

There also appeared to be slightly greater movement of the tracers on the lower side of the tablet – particularly, from the outer rim. (Note: each specimen was identified by lightly numbering the upper face, using a soft pencil; however, examination of horizontal slices from stacks of XμT data suggested that this had not affected the swelling.) Since each specimen was prepared by single-sided compaction, with a driven upper punch and static lower punch, the lower rim was expected to be of lower relative density, corresponding to a larger pore volume fraction [41–48]. Hence, these results suggested that variations in compaction pressure (and the resulting porosity) may affect swelling behaviour. (Note: in principle, XμT may be used to observe such density variations within tablets [49,50]; good quality analyses of this were not possible with the present data, however, due to increased greyscale variations (i.e. electronic 'noise') within pixels, as a consequence of the relatively short acquisition times used.)

Although the same RoI was selected throughout the swelling experiment, some of the original glass microsphere tracers seemed to be absent during later stages. This was caused by the tablet 'tilting' slightly during swelling, 'eliminating' tracers close to the front or rear limits of the RoI. These 'missing' tracers could be 'found' again by selecting a thicker RoI for the later images – but this also introduced other 'new' microspheres that were not present in the earlier images.

Closer examination of the XμT images revealed bands of lighter contrast that encroached into the cross-section from above and below. In order to examine this more clearly, Fig. 2 shows a set of frames, corresponding to the images in Fig. 1, that have been reanalysed using the 'Z Projection – maximum intensity' option to reveal regions of lighter pixels. It can be seen that these light bands formed parallel to the upper and lower faces, with roughly uniform thickness and contrast, at the start of swelling. Then, as swelling progressed, they thickened and expanded towards the centre of the specimen, eventually developing slightly thicker outer rims and meeting along the sides of the specimen. In some frames, the band close to the bottom of the tablet appeared slightly lighter; however, this was not significant given the contrast variations observable in the surrounding liquid. Attempts at more quantitative measurements (e.g. by plotting the pixel greyscale distributions) failed to reveal any systematic differences.

It is significant that these regions showed lighter X-ray absorbance contrast than the HPMC of the tablet or the surrounding water. A similar effect was also observed in our previous study [37]. In principle, this could occur in two ways: lower atomic number elements with fewer electrons have intrinsically lower X-ray absorbance and regions of lower mass density absorb X-rays less strongly. Clearly, there is no conceivable mechanism for the former, given the present experimental procedures; hence, it appears that the low absorbance contrast was due to regions of mass density lower than water. This suggested significant bubble formation within the swelling gel layer around the tablet, as reported previously [51–53]. The inability to resolve individual bubbles, in the present experiments, suggested relatively small sizes (i.e. 'microbubbles' with diameters less than 60 μm).

Several possible explanations for bubble formation during swelling can be proposed. Firstly, the water used to swell the specimens was expected to contain some dissolved gas, which may have come out of solution due to the gradual dissolution of HPMC. This explanation seems unlikely, however, since the light regions appeared to form within the region occupied by the swelling tablet – not the surrounding water. Instead, it seems more likely that the gas originated from air trapped within the specimen itself, in line with previous conclusions [51–53]. This suggested two further explanations. Trapped air that was compressed during compaction may have expanded as the HPMC softened, with the pressure causing the expansion. This, too, sounds unlikely, however, since the gas pressure would be exerted equally in all directions, causing both radial and axial expansion. It is also inconsistent with previous observations that the bubbles could be avoided simply by removing air from tablets under vacuum, prior to immersion in

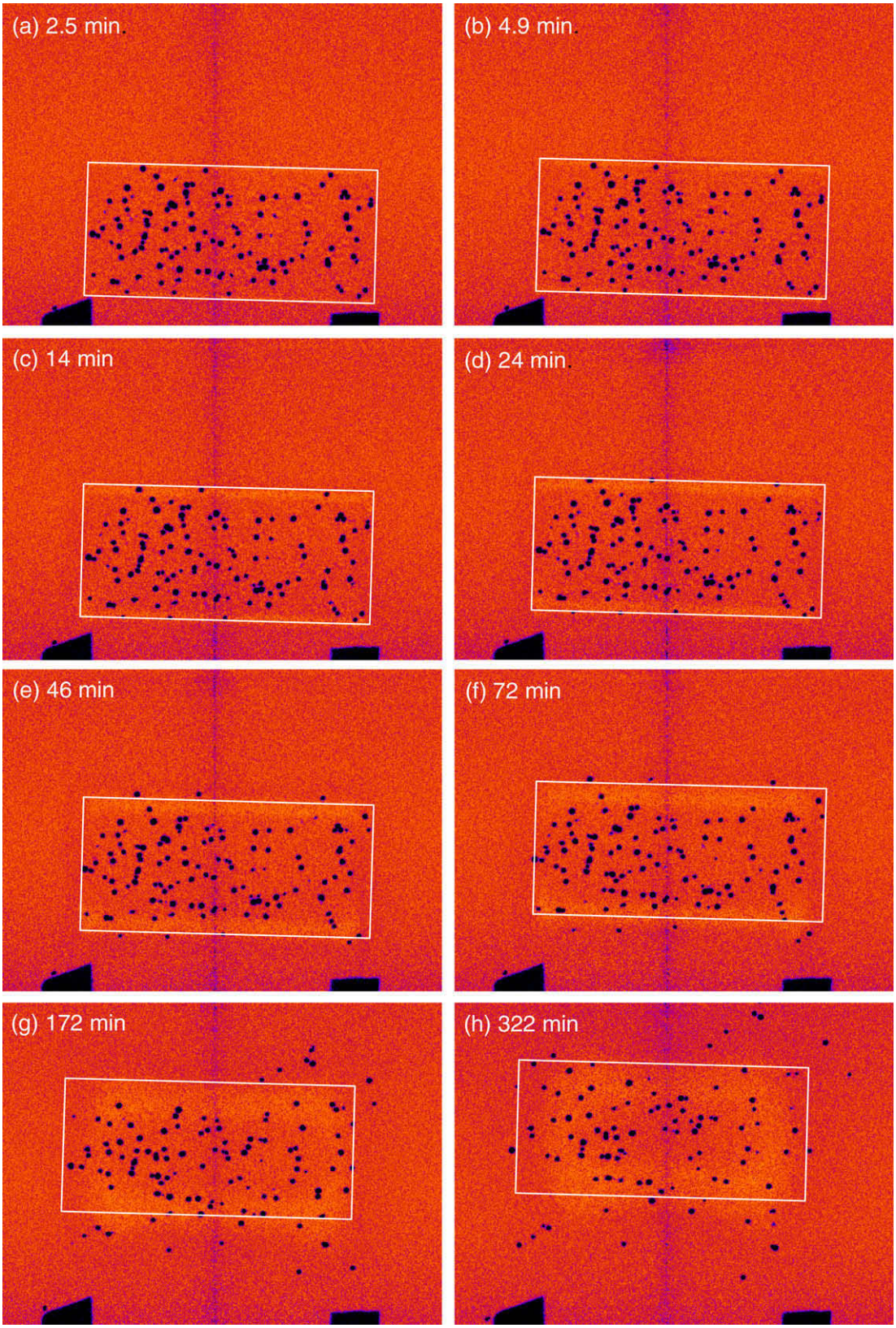

Fig. 1. Sequence of reconstructed vertical slices from XμT data, showing movement of glass microspheres during swelling, for HPMC specimen compacted at 127 MPa (rectangles indicate approximate initial size, vertical stripe through each image is an artefact). (For interpretation of the references to colour in this figure legend, the reader is referred to the web version of this article.)

water [53]. Moreover, it is expected that pressurised gas would find the easiest way out, leading to irregular 'jets' but little inflation. A more likely explanation is that residual stress in the compacted granules was able to relax as the HPMC became hydrated; the resulting mechanical expansion caused a pressure-decrease within the intergranular pores and bubble formation by the en-

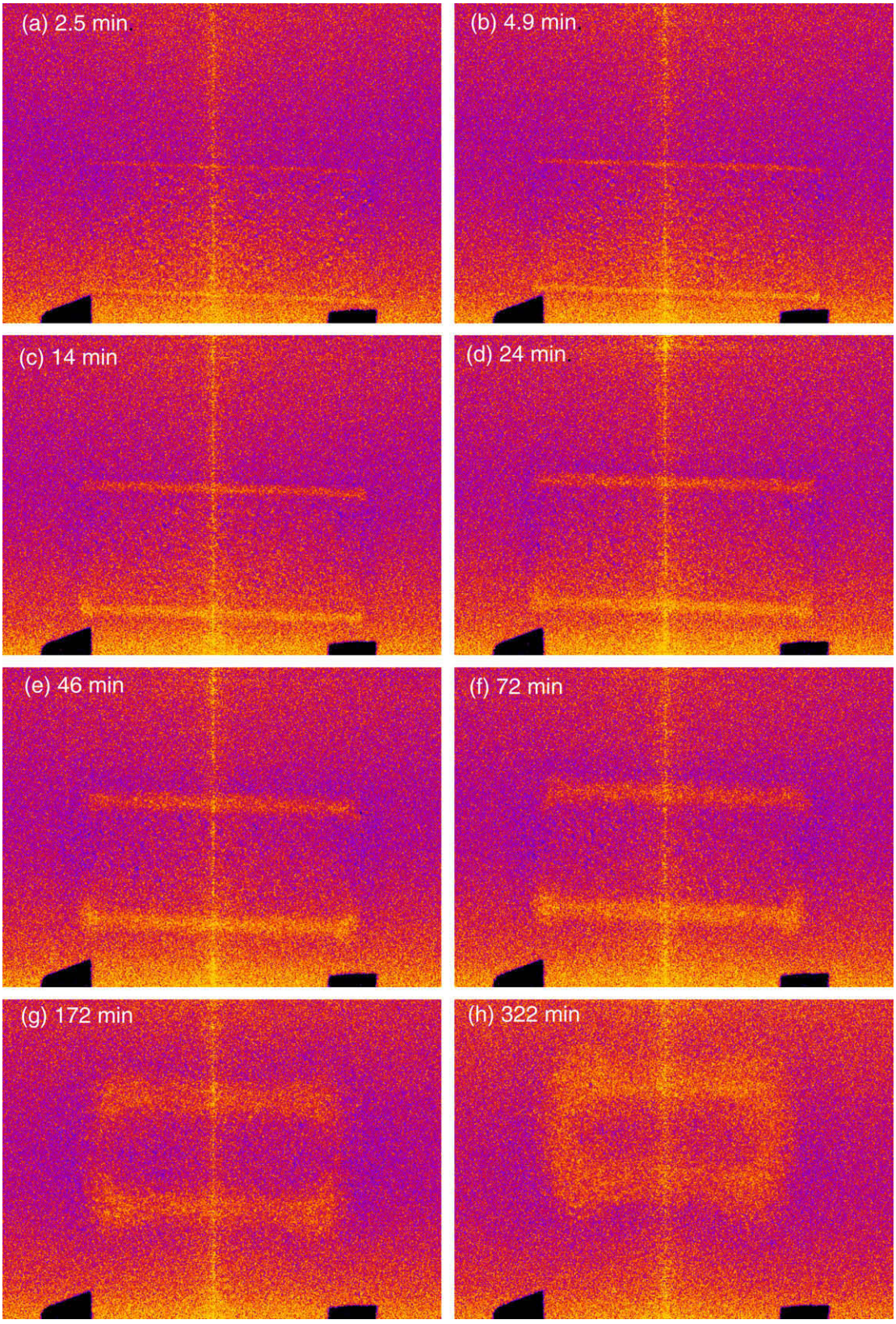

Fig. 2. Sequence of reconstructed vertical slices from XμT data, showing evolution of low density zone, during swelling for HPMC specimen compacted at 127 MPa. (For interpretation of the references to colour in this figure legend, the reader is referred to the web version of this article.)

trained air. Since the original compaction occurred axially, it seems reasonable that the relaxation should also occur in this direction.

Comparing the relative positions of the glass microspheres during swelling showed that arrival of the region of light contrast coincided with the start of axial expansion. This comparison is

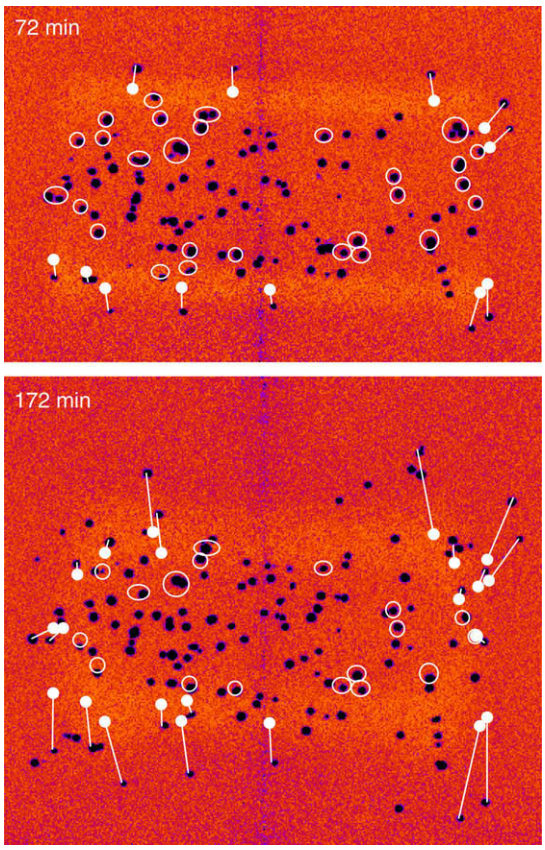

Fig. 3. Demonstrating relative displacement of glass microsphere tracers during swelling, for HPMC specimen compacted at 127 MPa (circles indicate features that have remained in the same relative position, neglecting upward movement due to swelling between tablet and support; relative movements are indicated by lines, from starting positions shown as white dots). (For interpretation of the references to colour in this figure legend, the reader is referred to the web version of this article.)

shown more clearly in Fig. 3. Selected microspheres that have remained in the same relative positions (i.e. neglecting the net upward movement due to swelling between tablet and support) are marked by circles; microsphere movements are shown by white lines linking the current locations to the starting positions, which are shown as white dots. Hence, it can be seen that microspheres within the 'core' (i.e. between the regions of lighter contrast) remained in the same relative configurations – with only a uniform upward movement, due to swelling between the tablet and support. Conversely, microspheres within or beyond the regions of lighter contrast showed considerable movement, which occurred predominantly in the axial direction – even when the tracer started close to the sides of the tablet. This suggested that the regions of lighter contrast were associated with 'expansion zones', within which relaxation of residual compaction stress occurred.

The 'core' thickness, $h_{core}(t)$, was measured manually, as the distance between the lighter 'expansion zones' in the projected image obtained from each XμT acquisition during the experiment. This process gave quite accurate measurements (±1 pixel equivalent to ±0.03 mm) during the early stages of swelling, where the light bands were of consistent thickness and the demarcation (i.e. absorbance contrast) from the rest of the tablet was sharp. During later stages of swelling, however, the thickness of the light bands became more irregular, and the demarcation from the 'core' became blurred; under these more difficult conditions, an uncertainty of ±6 pixels, corresponding to ±0.185 mm, was estimated for $h_{core}(t)$ close to the middle of the specimens (i.e. away from the corners, which thickened more). Plotting $h_{core}(t)$ against time revealed a dependence of the form:

$$h_{core}(t) = h_0 - kt^{1/2} \quad (1)$$

with k constant, as shown in Fig. 4a, where the error bars indicate the increasing uncertainty that was expected as the experiments progressed. Hence, plotting $h_{core}(t)$ against the square-root of time produced a straight line, as shown in Fig. 4b.

Although the expansion appeared to be initiated by water entering the HPMC, the precise hydration level at which it occurred was not determined, so the inner edge of the expansion zone may not be synonymous with the hydration front observable by MRI. (Indeed, it would be surprising if the water level required to initiate the mechanical relaxation coincided precisely with the MRI detection limit, which depends on water increasing the nuclear spin relaxation times sufficiently to acquire an echo signal above any background noise [21–23,37].) Nevertheless, based on the assumption that it occurred at a roughly constant water level, the observed inward advance of the expansion zone indicated water ingress, while the $t^{1/2}$-dependence suggested Fickian diffusion. Moreover, MRI studies frequently show that the water content rises steeply behind the hydration front [28,30–32,34,37]; consequently, estimating the position of the hydration front by XμT is less dependent on the precise water level at which the expansion started.

Since the core appeared to be eroded by two-sided diffusion (i.e. from above and below), an apparent diffusion constant could be estimated from:

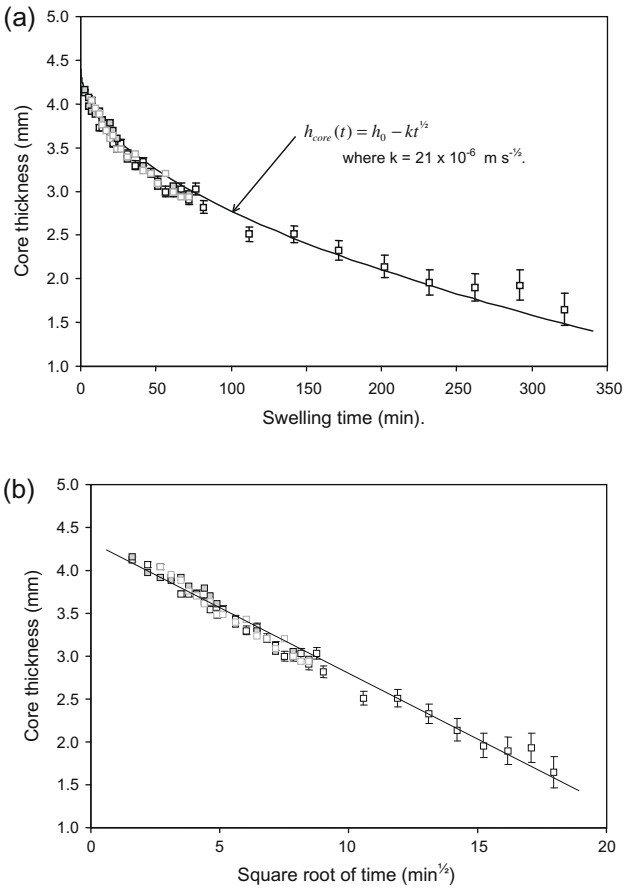

Fig. 4. Decrease in 'core' thickness during swelling, for HPMC compacted at 127 MPa (data measured in triplicate): (a) plotted vs. time; (b) vs. square-root of time.

$$D = \frac{k^2}{8} \quad (2)$$

For the data shown in Fig. 4, the constant (k =21 × 10^{-6} m $s^{-½}$) was equivalent to a diffusion coefficient of D = (0.055 ± 0.010) × 10^{-9} m^2 s^{-1}. These results agreed well with previous measurements of (radial) water penetration rates into HPMC using MRI, by Tritt-Goc and co-workers, which corresponded to Fickian diffusion with D in the range (0.02–0.06)×10^{-9} m^2 s^{-1}, depending on the swelling conditions and molecular weight of the HPMC [30,32]. Hence, this provides support for the assumption inherent in the present estimates of water penetration rates.

This interpretation of Fickian diffusion overlooks the effect of bubble formation in the expansion zone, however, which may affect the rate of water penetration by increasing tortuosity and reducing the cross-sectional area of the gel available for diffusion. Moreover, the occurrence of Fickian diffusion of water into HPMC seems rather surprising, in view of the significant increase in D with water content widely indicated by MRI diffusometry measurements [24,28,29]. Instead, it seems likely that the $t^{½}$-dependence of the core thickness may have occurred because the effects of bubble formation offset the increase in D expected with greater swelling.

Although slightly faster penetration may be expected in the radial, compared with the axial direction [32], estimates of (apparent) diffusion distances suggest that hydration of most material behind the flat faces occurred predominantly by axial penetration. This explains why the expansion zones remained essentially parallel to those faces for a considerable time, with deviations appearing first in the lower corners, where greater porosity was expected [41–48] to allow faster water penetration.

Combining the results from (axial) movements of the outermost tracers and the advancing expansion zones, close to the middle of the specimens, revealed the behaviour demonstrated in Fig. 5. The height increased, due to expansion of the gel layer, while the dry core between the advancing light bands (indicating expansion triggered by hydration) gradually became thinner. At the same time, only relatively small changes were observed in the radial direction. These results were qualitatively similar to previous observations of gel-layer formation, using MRI [37].

The effect of compaction pressure on the swelling behaviour of HPMC was investigated by comparing specimens prepared at 64 and 318 MPa. As shown in Table 1, the relative densities of the tablets increased with compaction pressure, in line with expectations. Since all the specimens were of roughly the same weight (0.40–0.41 g), the higher pressure samples were consequently thinner. Although the behaviour was qualitatively similar to that discussed previously for HPMC compacted at 127 MPa, the lower pressure specimens exhibited greater expansion while the higher pressure specimens expanded more slowly. This is demonstrated in Fig. 6a, by comparing the overall thickness estimated from the outermost tracer particles. These differences may be attributable to faster water penetration into the lower compaction pressure specimens, which were more porous. This hypothesis was supported by the apparent diffusion coefficients, estimated from the advancing light bands (expansion zones) for these specimens, as shown in Fig. 6b. This also corroborated previous observations of faster swelling from the lower (static punch) sides of specimens, which were expected to be of lower relative density, due to the effects of friction against the compaction die [41–48].

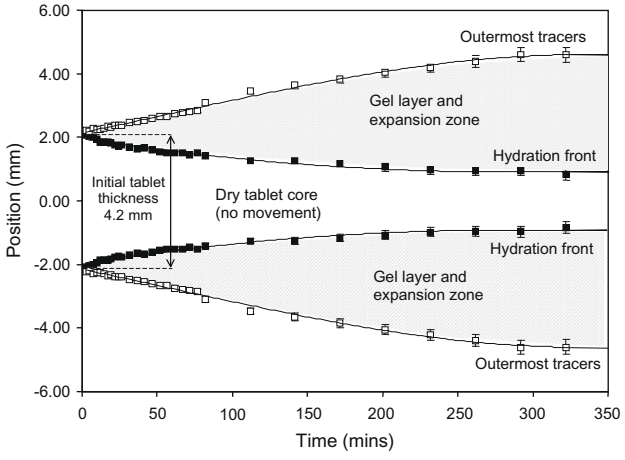

Fig. 5. Graph demonstrating water penetration and expansion during swelling, for HPMC specimen compacted at 127 MPa (shaded regions indicate gel).

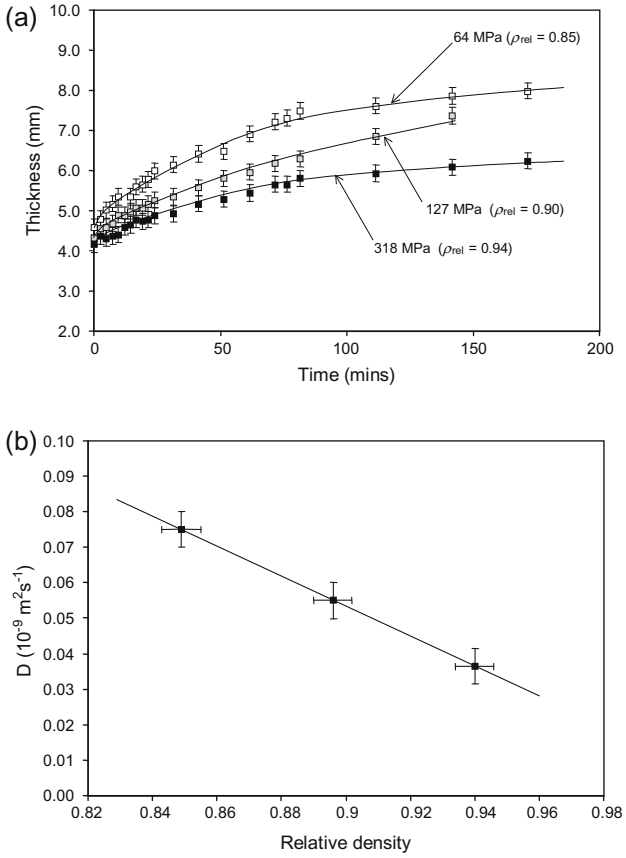

Fig. 6. Effect of compaction pressure for HPMC specimens: (a) expansion during swelling and (b) apparent diffusion coefficient for water penetration.

Incorporating MCC produced a small reduction in the relative densities of the tablets, suggesting that these formulations were less easily compacted than pure HPMC. Also, since MCC (1577 kg m^{-3} [44]) is more dense than HPMC (1335 kg m^{-3} [47]), using roughly the same weights of materials resulted in thinner specimens as the MCC content increased. Nevertheless, admixing up to 70% MCC appeared to have little effect on the expansion behaviour. Within the accuracy of the present experiments, the movements of tracer particles for the 10% MCC and 70% MCC specimens, shown in Fig. 7, appeared similar to the behaviour of 100% HPMC specimens.

By contrast, specimens made from 10% HPMC + 90% MCC expanded much more quickly, as shown in Fig. 8. Indeed, the rapid movement of tracer particles at the start of swelling prevented accurate reconstruction of the XμT data and produced the blurring in the first frame of Fig. 8; only those particles near the bottom of

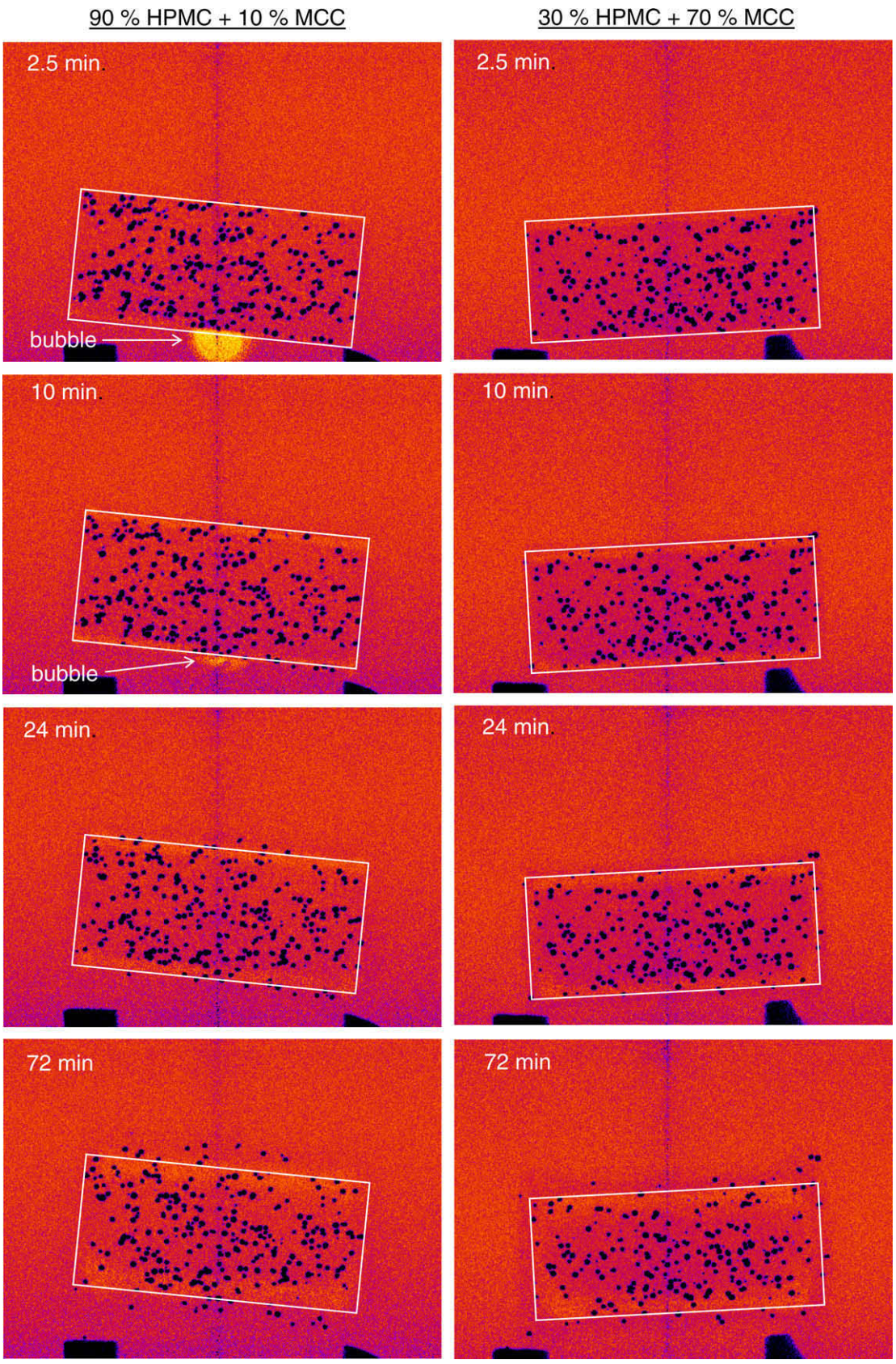

Fig. 7. Sequence of reconstructed vertical slices from XμT data, comparing the effect of composition, for HPMC–MCC mixture specimens (rectangles indicate approximate initial size, the light region below the 90% HPMC + 10% MCC specimen at the start of swelling was due to a trapped bubble). (For interpretation of the references to colour in this figure legend, the reader is referred to the web version of this article.)

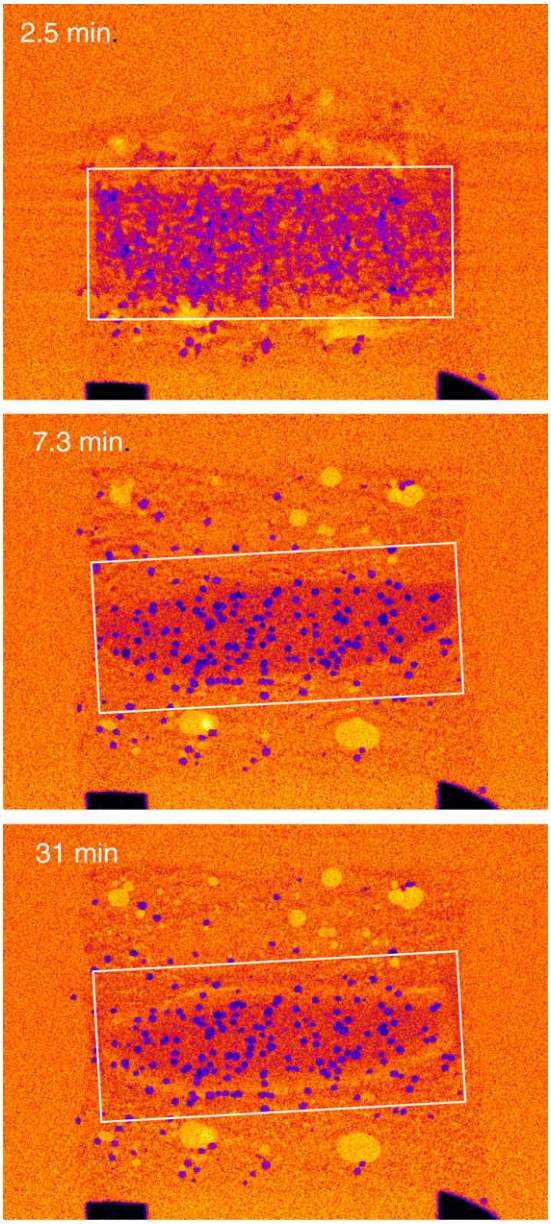

Fig. 8. Sequence of reconstructed vertical slices from XμT data, showing swelling behaviour of 10% HPMC + 90% MCC specimen, compacted at 127 MPa (rectangles indicate approximate initial size). (For interpretation of the references to colour in this figure legend, the reader is referred to the web version of this article.)

the specimen were sufficiently slow moving to be observed clearly. It was also very striking that the rapid expansion took place predominantly in the axial direction, with almost no increase in the diameter. Again, the most probable explanation would seem to be linked to mechanical relaxation of compaction stresses, while any inflation due to the pressure of trapped gas and simple gel formation by hydration of polymer chains would both be expected to occur more isometrically.

Higher MCC formulations were not investigated. It was noted, however, that tablets made of 100% MCC swelled rapidly and disintegrated completely within 1 min, which was too quick to study in the present experiments.

The formation of bubbles in the expansion zone was clearly observable for the 10% HPMC + 90% MCC formulation. In this case, it appeared that most of the trapped air coalesced into a few bubbles that were large enough to be resolved in the XμT images, with the

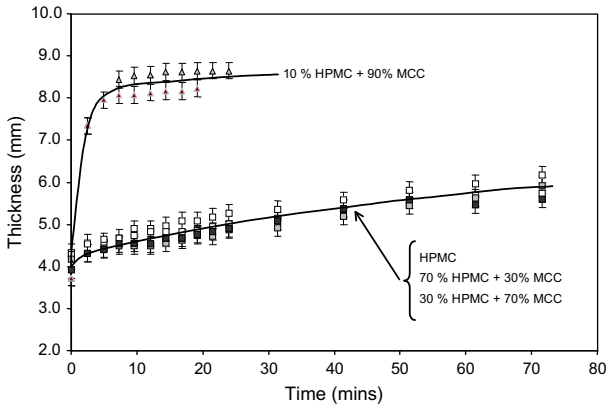

Fig. 9. Effect of composition on expansion behaviour, for HPMC + MCC mixtures.

largest approaching 1 mm diameter. Thin bands of unresolved, lighter contrast, suggestive of 'micro-bubbles' were also observable around the unswollen core, in the later frames of Fig. 8.

As shown in Fig. 9, the rapid expansion phase caused an approximate doubling of the specimen thickness (indicated by the outermost tracers) within the first 10 min of swelling. After 10 min,

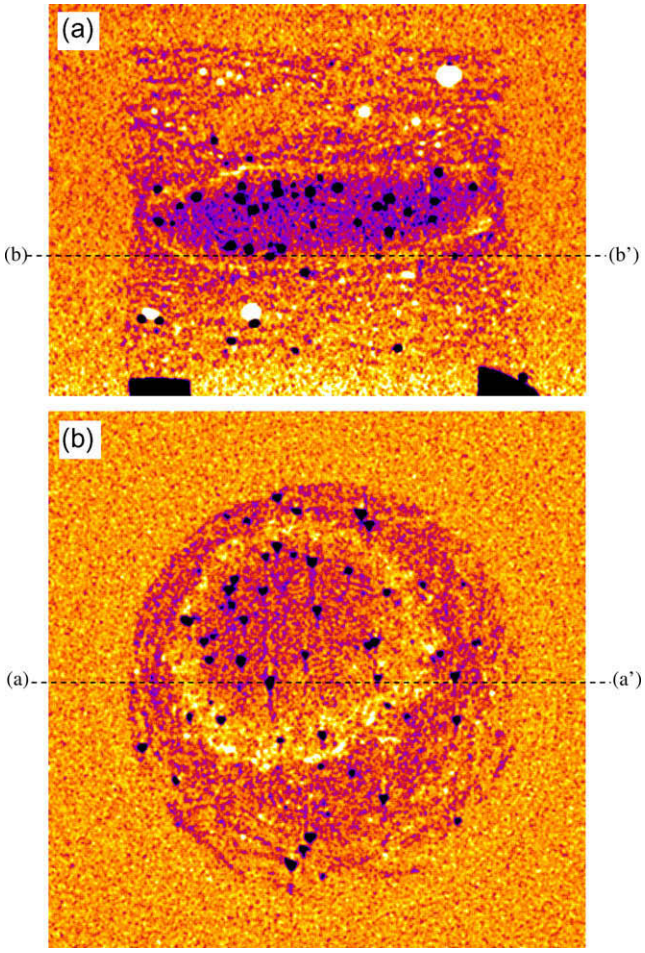

Fig. 10. High-contrast images from XμT data for 10% HPMC + 90% MCC specimen after 31-min swelling: (a) vertical slice in *xz*-plane through middle of swollen specimen and (b) horizontal slice in *xy*-plane, through lower interface between gel and unswollen core; the dashed lines (a–a') and (b–b') indicate where the images intersect each other. (For interpretation of the references to colour in this figure legend, the reader is referred to the web version of this article.)

however, the expansion slowed significantly, even though approximately half of the original tablet appeared to persist as a compacted core at the centre of the swollen specimen. Indeed, the subsequent expansion of the 10% HPMC + 90% MCC specimens appeared to be slower than that of the other formulations – although the overall thickness was still much larger.

A clear explanation for the decrease in expansion rate during the later stages of swelling is not currently known. One possibility may be that the gel layer had become sufficiently thick by this stage to control further water ingress and expansion. It seems unlikely, however, that a highly swollen, homogeneous gel containing MCC and HPMC in the same proportions as in the tablet would restrict further water ingress so effectively. Closer examination revealed that the gel was not homogeneous; images extracted from narrow regions (3 voxels thick) of the XμT data for a specimen after 31 min swelling (using 'Z Projection – average intensity', smoothing and high contrast) revealed distinct variations in the gel composition, as demonstrated in Fig. 10. Stratified layers of higher optical density were evident, along with the larger bubbles, in the gel layers above and below the tablet core. It seems likely that these denser regions may have been aggregates of MCC, which is not water-soluble, separating out from the aqueous HPMC gel. As noted previously, the limits of the unswollen tablet core appeared to be marked by a thin, light band, which suggested micro-bubble formation; this was also surrounded by a region of higher optical density approaching that of the tablet core, which suggested a high polymer concentration. Thus, the surface of the unswollen core may have become 'blinded' by a layer of MCC, in the same way that a filter can become blocked.

This effect may have been assisted by a pressure-decrease within the intergranular pores, caused by the expansion of the hydrated excipient particles, forcing the insoluble MCC into the interface. (This may be akin to the sucking effect of a syringe as the plunger is withdrawn.) Support for this hypothesis can be obtained from the fate of the bubble caught beneath the 90% HPMC + 10% MCC specimen, in Fig. 7. Close examination of successive XμT stacks

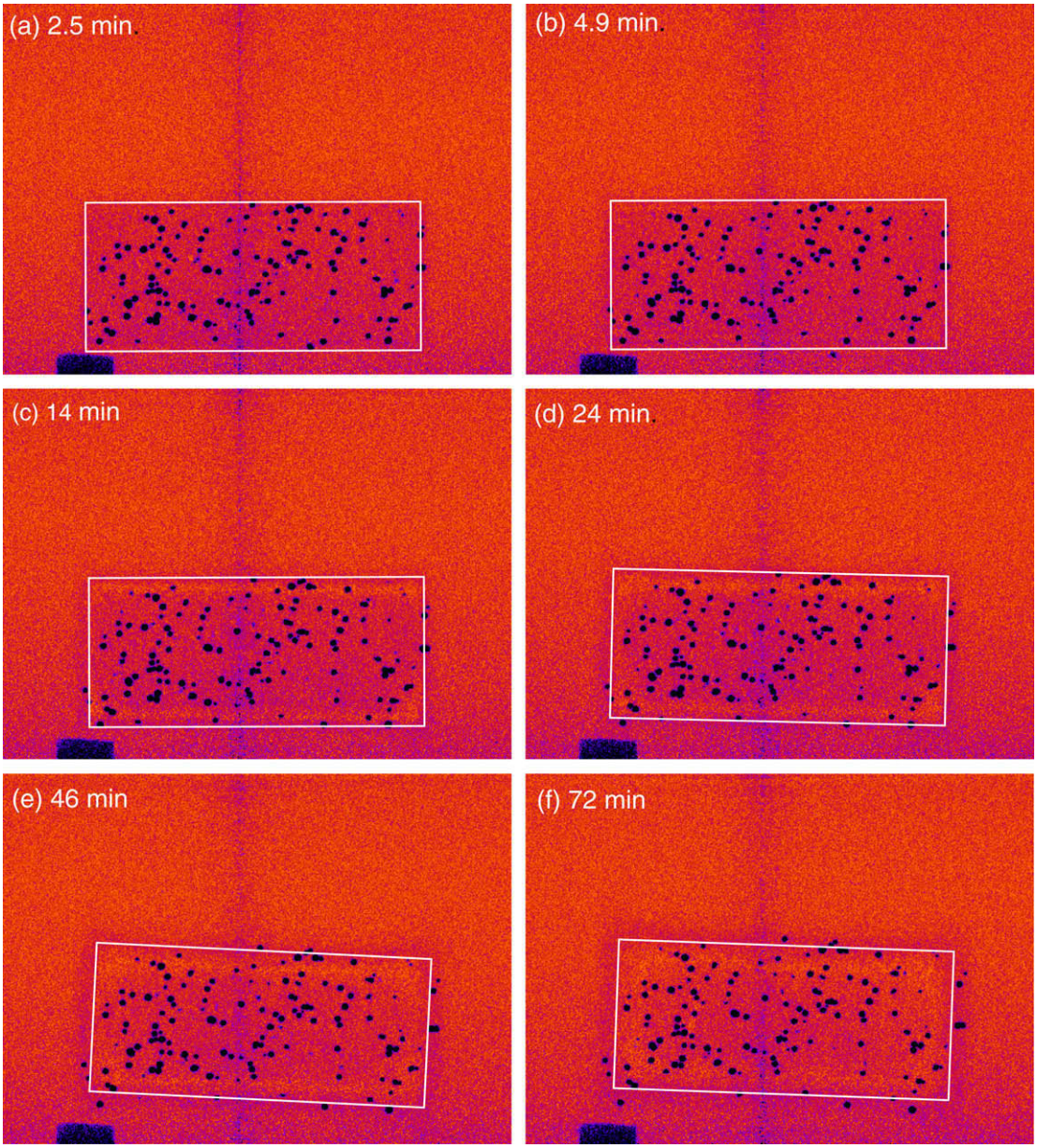

Fig. 11. Sequence of reconstructed vertical slices from XμT data, showing swelling behaviour of 10% HPMC + 90% PGS specimen, compacted at 127 MPa (rectangles indicate approximate initial size). (For interpretation of the references to colour in this figure legend, the reader is referred to the web version of this article.)

from the early part of this swelling experiment showed that the bubble remained beneath the tablet for at least 10 min. There was no indication that it was released by the sample-stage movements during the XμT acquisition, probably because it was trapped within gel; instead, the bubble became progressively smaller, suggesting that it had been gradually sucked into the underside of the expanding tablet. This observation raises a further question concerning the role of expansion during swelling – does it assist hydration by sucking water into the tablet?

The effect of substituting PGS for MCC was explored briefly. Fig. 11 shows the expansion behaviour of a 10% HPMC + 90% PGS specimen. Since PGS is also a gel-forming excipient, this formulation behaved roughly similar to HPMC or HPMC-rich mixtures. Movements of tracers suggested that axial expansion was less dominant during swelling, however, compared with HPMC or MCC, with radial expansion also evident within 14 min. Moreover, the light bands appeared rather less distinct above and below the core but extended around the sides of the tablet sooner, which also suggested that axial expansion was less dominant for the high PGS specimens compared with the other formulations investigated.

The most significant difference, however, was the formation of internal cracks within the 90% PGS specimen, after swelling for about 1 h, as shown in Fig. 12. These cracks exhibited light contrast (i.e. lower density than the water), suggesting that they were air-filled and, therefore, probably associated with expansion rather than water permeation. Since the three excipients used appeared

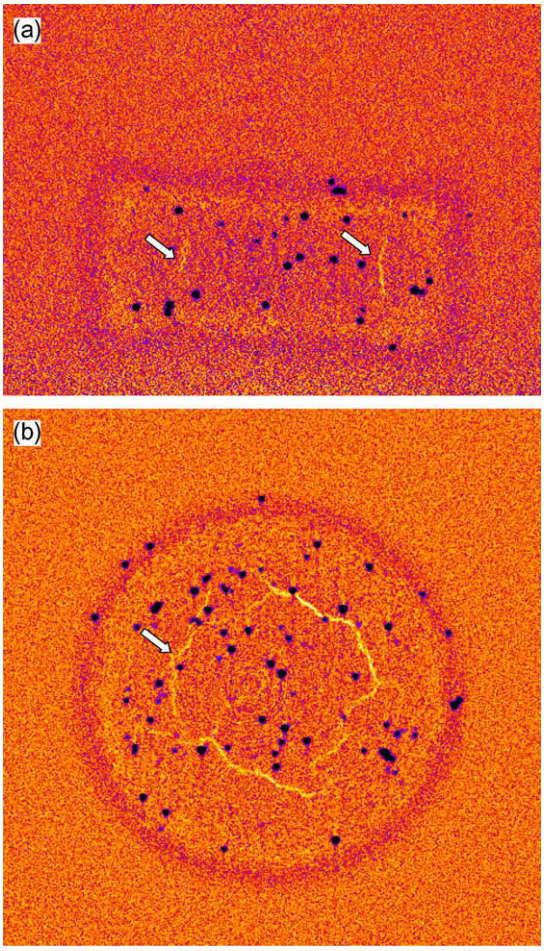

Fig. 12. Reconstructed vertical (a) and horizontal (b) slices, showing crack formed during swelling (after 60 min, for 10% HPMC + 90% PGS specimen, compacted at 127 MPa). (For interpretation of the references to colour in this figure legend, the reader is referred to the web version of this article.)

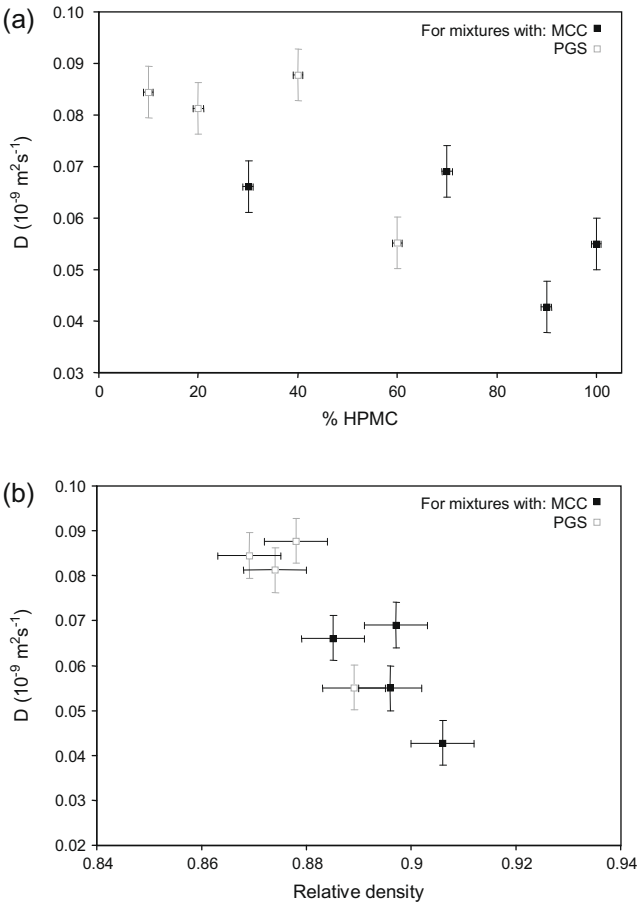

Fig. 13. Effect of composition on the apparent diffusion coefficient for water penetration, plotted against: (a) % HPMC in the formulation and (b) relative density of the compacted specimens.

to be similarly viscoelastic [47], it seemed unlikely that the cracks were due to more brittle behaviour of PGS compared with HPMC. Also, the cracking followed a roughly circular path, which would be consistent with radial swelling causing significant tension within the tablet. No comparable effects were observable for lower PGS formulations, however.

Changes in composition also appeared to produce small but systematic differences in the rates at which the expansion zones advanced into the specimens. Estimates of the apparent diffusion coefficient, shown in Fig. 13a, became smaller with increasing HPMC content, for mixtures with MCC or PGS. Although this may also reflect differences in the hydration behaviour of the materials, the main reason appeared to be related to changes in the relative densities (i.e. porosities) of the different formulations, as shown in Fig. 13b. This agreed with the expectation that the fastest water ingress would occur through the intergranular pores, rather than by diffusion through the excipient granules themselves, although the hydrophilicity of granule surfaces may play an important role.

4. Discussion

This work demonstrated a relatively new application of XμT to investigate tablet swelling behaviour, which followed on from our own 'pilot study' using a bench-top tomograph [37]. In the present work, the use of intense X-ray illumination from a synchrotron allowed good quality data to be collected relatively quickly, in order to investigate the early stages of swelling. Clearly, a method requiring synchrotron radiation cannot be easily used for routine appli-

cations. Nevertheless, the results from this work revealed interesting differences in tablet swelling behaviour, which were related to the compositions and compaction pressures used. Moreover, given the rapid advances in XμT systems over recent years [54], there is likely to be potential for wider application using bench-top instrumentation in the future.

Using XμT to follow the movements of tracer particles embedded within the tablets provided a clear demonstration of the dimensional changes that can occur within tablets during swelling. The most dramatic example was provided by the 10% HPMC + 90% MCC specimens, which doubled in thickness within a few minutes, while the diameters remained essentially unchanged; however, qualitatively similar behaviour was also evident with the other, more slowly swelling formulations. The dominance of axial expansion (i.e. the reverse of compaction) concurred with several previous reports [15,19,23,26,27,37] and has been attributed to 'mechanical relaxation' of residual compaction stress within the tablet.

Compaction experiments with viscoelastic materials such as HPMC, MCC and PGS generally reveal plastic deformation occurring under the effects of the applied force (i.e. creep) and elastic recovery (springback) during unloading [47,48,55–58]. Typically, the creep and springback correspond to a small part of the overall strain experienced by the powder bed during compaction. Moreover, despite these relaxation processes, compaction appears to produce an overall increase in internal energy [55–59], which may be able to drive further relaxation processes, given suitable conditions. Hence, further axial expansion appeared to be initiated by water ingress during swelling; this may occur concurrently, but it is distinct from swelling associated with the increase in polymer coil diameter caused by hydration. The latter process may be expected to produce more uniform, isotropic swelling so may have been responsible for the small amounts of radial expansion observed; it may also have been associated with the slower axial swelling of the 10% HPMC + 90% MCC specimens, after the rapid initial phase.

Further work is required to fully explain the mechanisms involved in the axial expansion. The need for water ingress seems quite clear; expansion proceeded quite rapidly after the tablets were immersed, although no significant dimensional changes had occurred between compacting powders to prepare the specimens and starting the experiments (a period of approximately 2 weeks). It is not clear, however, whether the role of water was to plasticise the excipient within the compacted granules, to reduce intergranular attraction by hydrating surfaces within or between granules, to 're-inflate' pores that had been collapsed during tabletting, or some other process.

Ideally, a method for observing the swelling effects caused by chain solvation and mechanical relaxation separately would be useful. In this respect, it may be very informative to compare observations of swelling using XμT with spatially resolved measurements of water concentrations from other methods such as MRI, along the lines reported previously [37]. This would constitute an important subject for further experimentation but is beyond the scope of the present work.

Clearly, the choice of excipients can have a considerable effect on the swelling and disintegration behaviour of tablets. The work reported here demonstrates how more subtle control of the swelling behaviour can be achieved by using combinations of excipients. Hence, as an example, the swelling behaviour was faster in tablets with more MCC, although this change was clearly not linear – the behaviour remained fairly constant up to 70% MCC but then increased rapidly for higher MCC formulations. It seems likely that this change in behaviour resulted from the balance between the gel-forming HPMC and the rapidly disintegrating MCC. Several authors have applied percolation theory to account for changes in tablet properties with composition [60–63]. Since the percolation threshold for three-dimensional systems of similarly sized granules is expected to be in the range 0.15–0.25 [63], this may offer an explanation for the much faster swelling rates observed for the 90% MCC specimens, where the HPMC particles formed isolated clusters. Also, this formulation may have contained insufficient HPMC to rapidly form a surface gel that could control subsequent water ingress, along the lines suggested elsewhere [18,19].

It also appeared that the swelling behaviour could be affected by pressing conditions. This was consistent with expectations, since increased compaction force produces tablets with higher density (i.e. lower pore volume), which may reduce the rate of water ingress, to initiate the swelling process. As a consequence of density variations within tablets, which occur due to the effects of wall friction during compaction [41–48], it also appears that there may be local differences in swelling rates within a single tablet.

The most important observation, however, concerns the formation of bubbles within the expansion zones. This phenomenon has been reported previously by several workers [51–53]. Indeed, Korsmeyer et al. [51] suggested that this would affect the drug-delivery characteristics, *in vivo*, by making tablets more buoyant. Also, Fyfe and Blazek [53] attributed an overestimate of HPMC content in their MRI experiments to bubbles occupying part of the gel layer around a swelling tablet (i.e. increasing the volume of gel, while being unobserved in the MRI). Nevertheless, the presence of bubbles appears to have been overlooked in previous attempts to measure diffusion rates. Clearly, bubbles are expected to occlude part of the gel and increase the tortuosity of diffusion paths, which would reduce the rate of water penetration into tablets. Since these effects may offset the expected increase in D with hydration in gel-forming excipients, this may cause apparently Fickian diffusion in what is really a Case II system. A more detailed treatment is beyond the scope of the present report but should be addressed in future work.

Other than our own 'pilot study' using a bench-top tomograph [37], the work reported here is the first application of XμT to investigate swelling behaviour of different tablet formulations. Consequently, while this technique shows considerable promise, it is not surprising that several 'loose ends' and unresolved questions remain. For example, it would be interesting to explore the change in behaviour from 'gradual' to 'rapid' swelling that occurred somewhere between 70% and 90% MCC in HPMC, in order to test the percolation theory explanation more thoroughly. It would also be interesting to extend the range of concentrations examined to include ternary mixtures of HPMC, MCC and PGS, as well as other common excipients. These issues should be considered in further work.

5. Conclusions

The potential of XμT for studying tablet swelling was demonstrated. Using intense X-ray illumination from a synchrotron source permitted rapid data acquisition, so that the early stages of swelling behaviour could be followed in 'real time'. This revealed several differences due to excipient type and compaction conditions.

In all cases, significant axial expansion was observed, which may be due to mechanical relaxation of residual compaction stress. This expansion appeared to be accompanied by extensive bubble formation, which may have significantly affected water penetration rates into the tablets. More detailed analyses of these phenomena, including the role played by water in initiating these processes, are beyond the scope of the present report but merit further investigation.

Acknowledgements

The authors would like to thank the staff of the ESRF who made this work possible, especially Dr. Elodie Boller for invaluable help in setting up beamline ID19 and converting the projected images to XμT data stacks. We are also very grateful to the ESRF and Pfizer PLC., for financial support and to Dr. Xiaowei Fu for practical help in performing the experiments. The authors would also like to acknowledge the thought-provoking comments and questions raised by the (anonymous) reviewers of this paper.

References

[1] M.E. Aulton, Pharmaceutics: The Science of Dosage Form Design, second ed., Churchill Livingstone, Edinburgh, 2002.
[2] A.M. Hillery, A.W. Lloyd, J. Swarbrick (Eds.), Drug Delivery and Targeting for Pharmacists and Pharmaceutical Scientists, Taylor and Francis, London, 2001.
[3] M.N.V.R. Kumar, N. Kumar, Polymeric controlled drug-delivery systems: perspective issues and opportunities, Drug Dev. Ind. Pharm. 27 (2001) 1–30.
[4] S. Zuleger, B.C. Lippold, Polymer particle erosion controlling drug release. I. Factors influencing drug release and characterisation of the release mechanism, Int. J. Pharm. 217 (2001) 139–152.
[5] M.J. Vázquez, B. Pérez-Marcos, J.L. Gómez-Amoza, R. Martínez-Pacheco, Influence of technological variables on release of drugs from hydrophilic matrices, Drug Dev. Ind. Pharm. 18 (1992) 1355–1375.
[6] C.D. Melia, Hydrophilic matrix sustained-release systems based on polysaccharide carriers, Crit. Rev. Therap. Drug Carrier Syst. 8 (1991) 395–421.
[7] J. Siepmann, N.A. Peppas, Modelling of drug release from delivery systems based on hydroxypropyl methyl cellulose (HPMC), Adv. Drug Dev. Rev. 48 (2001) 139–157.
[8] J. Nerurkar, H.W. Jun, J.C. Price, M.O. Park, Controlled-release matrix tablets of ibuprofen using cellulose ethers and carrageenans: effect of formulation factors on dissolution rates, Eur. J. Pharm. Biopharm. 61 (2005) 56–68.
[9] P. Colombo, R. Bettini, P. Santi, N.A. Peppas, Sellable matrices for controlled drug delivery: gel-layer behaviour, mechanisms and optimal performance, Pharm. Sci. Technol. Today 3 (2000) 198–204.
[10] S. Kiortsis, K. Kachrimanis, T. Broussali, S. Malamataris, Drug release from tabletted wet granulations comprising cellulosic (HPMC or HPC) and hydrophobic component, Eur. J. Pharm. Biopharm. 59 (2005) 73–83.
[11] N.K. Ebube, A.B. Jones, Sustained release of acetaminophen from a heterogeneous mixture of two hydrophilic non-ionic cellulose ether polymers, Int. J. Pharm. 272 (2004) 19–27.
[12] D.S. Roy, B.D. Rohera, Comparative evaluation of rate of hydration and matrix erosion of HEC and HPC and study of drug release from their matrices, Eur. J. Pharm. Sci. 16 (2002) 193–199.
[13] R.O. Williams, T.D. Reynolds, T.D. Cabelka, M.A. Sykora, V. Mahaguna, Investigation of excipient type and level on drug release from controlled release tablets containing HPMC, Pharm. Dev. Technol. 7 (2002) 181–193.
[14] M. Levina, A.R. Rajabi-Siahboomi, The influence of excipients on drug release from hydroxypropyl methylcellulose matrices, J. Pharm. Sci. 93 (2004) 2746–2754.
[15] M. Efentakis, I. Pagoni, M. Vlachou, K. Avgoustakis, Dimensional changes, gel layer evolution and drug release studies in hydrophilic matrices loaded with drugs of different solubility, Int. J. Pharm. 339 (2007) 66–75.
[16] C. Ferrero, A. Mũnoz-Ruis, M.R. Jiménez-Castellanos, Fronts movement as a useful tool for hydrophilic matrix release mechanism elucidation, Int. J. Pharm. 202 (2000) 21–28.
[17] J.J. Escudero, C. Ferrero, M.R. Jiménez-Castellanos, Compaction properties, drug release kinetics and fronts movement studies from matrices combining mixtures of swellable and inert polymers: effect of HPMC of different viscosity grades, Int. J. Pharm. 351 (2008) 61–73.
[18] G. Bajwa, H. Hoebler, C. Sammon, P. Timmins, C.D. Melia, Microstructural imaging of early gel layer formation in HPMC matrices, J. Pharm. Sci. 95 (2006) 2145–2157.
[19] P. Gao, R.H. Meury, Swelling of hydroxypropyl methylcellulose matrix tablets. 1. Characterisation of swelling using a novel optical imaging method, J. Pharm. Sci. 85 (1996) 725–731.
[20] J. Adler, A. Jayan, C.D. Melia, A method for quantifying differential expansion within hydrating hydrophilic matrixes by tracking embedded fluorescent microspheres, J. Pharm. Sci. 88 (1999) 371–377.
[21] J.C. Richardson, R.W. Bowtell, K. Mäder, C.D. Melia, Pharmaceutical applications of magnetic resonance imaging (MRI), Adv. Drug Deliv. Rev. 57 (2005) 1191–1209.
[22] C.D. Melia, Rajabi-Siahboomi, R.W. Bowtell, Magnetic resonance imaging of controlled release pharmaceutical dosage forms, Pharm. Sci. Technol. Today 1 (1998) 32–39.
[23] A.R. Rajabi-Siahboomi, R.W. Bowtell, P. Mansfield, A. Henderson, M.C. Davies, C.D. Melia, Structure and behaviour in hydrophilic matrix sustained-release dosage forms: 2. NMR-imaging studies of dimensional changes in the gel layer and core of HPMC tablets undergoing hydration, J. Control. Release 31 (1994) 121–128.
[24] A.R. Rajabi-Siahboomi, R.W. Bowtell, P. Mansfield, M.C. Davies, C.D. Melia, Structure and behaviour in hydrophilic matrix sustained-release dosage forms: 4. Studies of water mobility and diffusion coefficients in the gel layer of HPMC tablets using NMR imaging, Pharm. Res. 13 (1996) 376–380.
[25] M. Ashraf, V.L. Iuorno, D. Coffinbeach, C.A. Evans, L.L. Augsburger, A novel nuclear-magnetic resonance (NMR) imaging method for measuring the water front penetration rate in hydrophilic polymer matrix capsule plugs and its role in drug release, Pharm. Res. 11 (1994) 733–737.
[26] M. Kojima, S. Ando, K. Kataoka, T. Hirota, K. Aoyagi, H. Nakagami, Magnetic resonance imaging (MRI) study of swelling and water mobility in micronized low-substituted hydroxypropylcellulose matrix tablets, Chem. Pharm. Bull. 46 (1998) 324–328.
[27] M. Kojima, H. Nakagami, Investigation of water mobility and diffusivity in hydrating micronized low-substituted hydroxypropyl cellulose, hydroxypropyl methyl cellulose, and hydroxypropyl cellulose matrix tablets by magnetic resonance imaging (MRI), Chem. Pharm. Bull. 50 (2002) 1621–1624.
[28] C.A. Fyfe, A.I. Blazek, Investigation of hydrogel formation from hydroxypropyl methylcellulose (HPMC) by NMR spectroscopy and NMR imaging techniques, Macromolecules 30 (1997) 6230–6237.
[29] C.A. Fyfe, A.I. Blazek-Welsh, Quantitative NMR imaging study of the mechanism of drug release from swelling hydroxypropylmethylcellulose tablets, J. Control. Release 68 (2000) 313–333.
[30] J. Tritt-Goc, N. Pislewski, Magnetic resonance imaging study of the swelling kinetics of hydroxypropylmethylcellulose in water, J. Control. Release 80 (2002) 79–86.
[31] J. Kowalczuk, J. Tritt-Goc, N. Pislewski, The swelling properties of hydroxypropyl-methyl-cellulose loaded with tetracycline hydrochloride: magnetic resonance imaging study, Solid State Nucl. Mag. Res. 25 (2004) 35–41.
[32] J. Tritt-Goc, J. Kowalczuk, Spatially resolved solvent interaction with glassy HPMC polymers studied by magnetic resonance microscopy, Solid State Nucl. Mag. Res. 28 (2005) 250–257.
[33] S. Baumgartner, G. Lahajnar, A. Sepe, J. Kristl, Quantitative evaluation of polymer concentration profile during swelling of hydrophilic matrix tablets using ^{1}H NMR and MRI methods, Eur. J. Pharm. Biopharm. 59 (2005) 299–306.
[34] W.E. Baille, C. Malveau, X.X. Zhu, R.H. Marchessault, NMR imaging of high-amylose starch tablets. 1. Swelling and water uptake, Biomacromolecules 3 (2002) 214–218.
[35] C. Malveau, W.E. Baille, X.X. Zhu, R.H. Marchessault, NMR imaging of high-amylose starch tablets. 2. Effect of tablet size, Biomacromolecules 3 (2002) 1249–1254.
[36] C. Dahlberg, A. Fureby, M. Schuleit, S.V. Dvinskikh, I. Furó, Polymer mobilisation and drug release during tablet swelling. A ^{1}H NMR and NMR microimaging study, J. Control. Release 122 (2007) 199–205.
[37] P.R. Laity, M.D. Mantle, L.F. Gladden, R.E. Cameron, Magnetic resonance imaging and X-ray microtomography studies of a gel-forming tablet formulation, Eur. J. Pharm. Biopharm. 74 (2010) 109–119.
[38] J.-C. Labiche, O. Mathon, S. Pascarelli, M.A. Newton, G.G. Ferre, C. Curfs, G. Vaughan, A. Homs, The fast readout low noise camera as a versatile X-ray detector for time resolved dispersive extended X-ray absorption fine structure and diffraction studies of dynamic problems in materials science, chemistry, and catalysis, Rev. Sci. Instrum. 78 (2007) 091301.
[39] Technical information available from ESRF website. <http://www.esrf.eu/UsersAndScience/Experi-ments/Imaging/ID22/BeamlineManual/Detectors/Ccd/Frelon>.
[40] More information on Image-J and software downloads are available at: <http://rsbweb.nih.gov/ij/>.
[41] B. Eiliazadeh, B.J. Briscoe, Y. Sheng, K. Pitt, Investigating density distributions for tablets of different geometry during the compaction of pharmaceuticals, Particul. Sci. Technol. 21 (2003) 303–316.
[42] A. Kandeil, M.C. de Malherbe, The use of hardness in the study of compaction behaviour and die loading, Powder Technol. 17 (1977) 253–257.
[43] C.-Y. Wu, O.M. Ruddy, A.C. Bentham, B.C. Hancock, S.M. Best, J.A. Elliott, Modelling the mechanical behaviour of pharmaceutical powders during compaction, Powder Technol. 152 (2005) 107–117.
[44] L.H. Han, J.A. Elliott, A.C. Bentham, A. Mills, G.E. Amidon, B.C. Hancock, A modified Drucker–Prager Cap model for die compaction simulation of pharmaceutical powders, Int. J. Solids Struct. 45 (2008) 3088–3106.
[45] H.S. Kim, Densification modelling for nanocrystalline metallic powders, J. Mater. Process. Technol. 140 (2003) 401–406.
[46] R.J. Crawford, D.W. Paul, D. Sprevak, Solid phase compaction of polymeric powders: effects of compaction conditions on pressure and density variations, Polymer 23 (1982) 123–128.
[47] P.R. Laity, R.E. Cameron, A small-angle X-ray scattering study of powder compaction, Powder Technol. 188 (2008) 119–127.
[48] P.R. Laity, R.E. Cameron, A small-angle X-ray scattering study of local variations within powder compacts, Powder Technol. 192 (2009) 287–297.
[49] I.C. Sinka, S.F. Burch, J.H. Tweed, J.C. Cunningham, Measurement of density variations in tablets using X-ray computed tomography, Int. J. Pharm. 271 (2004) 215–224.
[50] V. Busignies, B. Leclerc, P. Porion, P. Evesque, G. Couarraze, P. Tchoreloff, Quantitative measurements of localized density variations in cylindrical tablets using X-ray microtomography, Eur. J. Pharm. Biopharm. 64 (2006) 38–50.
[51] R.W. Korsmeyer, R. Gurny, E. Doelker, P. Buri, A. Peppas, Mechanisms of potassium chloride release from compressed hydrophilic polymeric matrices: effect of entrapped air, J. Pharm. Sci. 72 (1983) 1189–1191.

[52] C.D. Melia, A.R. Rajabi-Siahboomi, A.C. Hodson, J. Adler, J.R. Mitchell, Structure and behaviour of hydrophilic matrix sustained release dosage forms: 1. The origin and mechanism of formation of gas bubbles in the hydrated surface layer, Int. J. Pharm. 100 (1993) 263–269.
[53] C.A. Fyfe, A.I. Blazek, Complications in investigations of the swelling of hydrogel matrices due to the presence of trapped gas, J. Control. Release 52 (1998) 221–225.
[54] S.R. Stock, Recent advances in X-ray microtomography applied to materials, Int. Mater. Rev. 53 (2008) 129–181.
[55] K. Van der Voort Maarschalk, K. Zuurman, H. Vromans, G.K. Bolhuis, C.F. Lerk, Stress relaxation of compacts produced from viscoelastic materials, Int. J. Pharm. 151 (1997) 27–34.
[56] K. Van der Voort Maarschalk, H. Vromans, W. Groenendijk, G.K. Bolhuis, C.F. Lerk, Effect of water on deformation and bonding of pregelatinized starch compacts, Eur. J. Pharm. Biopharm. 44 (1997) 253–260.
[57] B. Van Veen, K. Van der Voort Maarschalk, G.K. Bolhuis, M.R. Visser, K. Zuurman, H.W. Frijlink, Pore formation in tablets compressed from binary mixtures as a result of deformation and relaxation of particles, Eur. J. Pharm. Sci. 15 (2002) 171–177.
[58] V. Busignies, B. Leclerc, P. Porion, P. Evesque, G. Couarraze, P. Tchoreloff, Compaction behaviour and new predictive approach to the compressibility of binary mixtures of pharmaceutical excipients, Eur. J. Pharm. Biopharm. 64 (2006) 66–74.
[59] A. Zavaliangos, S. Galen, J. Cunningham, D. Winstead, Temperature evolution during compaction of pharmaceutical powders, J. Pharm. Sci. 97 (2008) 3291–3304.
[60] V. Busignies, B. Leclerc, P. Porion, P. Evesque, G. Couarraze, P. Tchoreloff, Application of percolation model to the tensile strength and the reduced modulus of elasticity of three compacted pharmaceutical excipients, Eur. J. Pharm. Biopharm. 67 (2007) 507–514.
[61] V. Busignies, B. Leclerc, P. Porion, P. Evesque, G. Couarraze, P. Tchoreloff, Investigation and modelling approach of the mechanical properties of compacts made with binary mixtures of pharmaceutical excipients, Eur. J. Pharm. Biopharm. 64 (2006) 51–65.
[62] G. Kimura, M. Puchkov, G. Betz, H. Leuenberger, Percolation theory and the role of maize starch as a disintegrant for a low water-soluble drug, Pharm. Dev. Technol. 12 (2007) 11–19.
[63] H. Leuenberger, The application of percolation theory in powder technology, Adv. Powder Technol. 10 (1999) 323–352.